Available online at www.sciencedirect.com
ScienceDirect
Bioorganic & Medicinal Chemistry 15 (2007) 4741–4752
Bioorganic & Medicinal Chemistry

Exploring DNA topoisomerase I inhibition by the benzo[*c*]phenanthridines fagaronine and ethoxidine using steered molecular dynamics

Rachel L. Clark,[a] Fiona M. Deane,[b] Nahoum G. Anthony,[a] Blair F. Johnston,[a] Florence O. McCarthy[b] and Simon P. Mackay[a,*]

[a]*Strathclyde Institute for Pharmacy and Biomedical Sciences, University of Strathclyde, 27 Taylor Street, Glasgow G4 0NR, UK*
[b]*Department of Chemistry and ABCRF, University College Cork, Western Road, Cork, Ireland*

Received 26 October 2006; accepted 2 May 2007
Available online 6 May 2007

Abstract—The benzo[*c*]phenanthridines (BCPs) are a group of compounds that are believed to express their antitumor activity through the inhibition of topoisomerase I. The enzyme is crucial to cell cycle division and progression, and regulates the equilibrium between relaxed and supercoiled DNA that occurs during DNA replication. Over the years, we have prepared a number of BCPs and employed a number of biophysical techniques to explore their mechanism of action and improve their activity against this particular enzyme. The naturally occurring alkaloid fagaronine **1** and the synthetic compound ethoxidine **3** are two of the most active compounds, although their inhibitory mechanisms are different, being a poison and suppressor, respectively. We have modified the approach of steered molecular dynamics to create a torque on the intercalator to comprehensively sample the DNA binding site, and using topoisomerase I crystal structures, have proposed a model to explain the different mechanisms of action for these two BCP compounds.

1. Introduction

DNA topoisomerase I (topo I) is an essential enzyme that controls DNA supercoiling and torsional strain during processes such as replication, transcription, and DNA repair. The catalytic intermediate of topo I is the cleavable complex which consists of a DNA single-strand break where the enzyme has become covalently linked to the 3′-terminus of the cleaved DNA by nucleophilic attack between the enzyme catalytic tyrosine and the phosphate in the scissile strand.[1] DNA topo I has been recognized as a key target for the camptothecin class of anticancer drugs presently used in the clinic.[2] In general, the drugs convert the enzyme into a cellular poison by stabilizing the topoisomerase cleavable complex. The resulting stabilized covalent intermediates are presumed to form obstacles to the advancement of the transcription and replication complexes that eventually lead to cell damage and cell death.[3] Trapping of the complex occurs when the religation step between the 5′-hydroxyl and the 3′-phosphotyrosine is impaired.[4] Since topo I is a target for these drugs,[2] these recent clinical findings emphasize the need for a thorough understanding of the action of the drugs at the molecular level. The structural information released by the recent publication of the ternary crystal structures for topo I and DNA with a variety of poisons[5,6] should provide the impetus for the discovery of new anticancer drugs.

The BCPs are naturally occurring isoquinoline alkaloids with numerous biological activities[7] that exert two types of inhibitory activity against topo I; poisoning and/or suppression. The differences in substituent nature and arrangement around the core heterocyclic ring system for the various BCPs give rise to this mechanistic duality. Fagaronine **1**, isolated from the roots of *Fagara zanthoxyloides* Lam. (Rutaceae), is a DNA intercalating agent[8,9] and a potent topo I poison stabilizing the topo I cleavable complex at low concentrations in a typical camptothecin-dependent manner.[4] The structurally related indenoisoquinolines NSC314622 **2a** and Mj-II-38 **2b** and their analogues developed by Cushman's

Keywords: Benzo[*c*]phenanthridine; Topoisomerase; Intercalator; Molecular dynamics.
* Corresponding author. Tel.: +44 (0) 141 548 2866; fax: +44 (0) 141 552 6443; e-mail: simon.mackay@strath.ac.uk

0968-0896/$ - see front matter © 2007 Elsevier Ltd. All rights reserved.
doi:10.1016/j.bmc.2007.05.002

group are also topo I poisons.[10–12] At higher levels fagaronine suppresses topo I and II complex formation[13–16] which in itself is not an unusual phenomenon, given that topo I cleavable complex suppression is observed at the high drug concentrations associated with multiple intercalative binding and significant DNA helical distortions.[16–18]

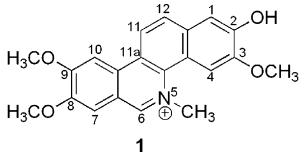

1

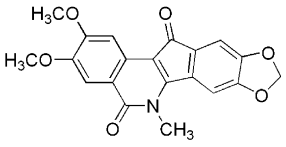

2a

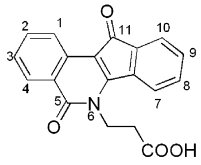

2b

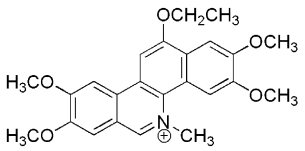

3

We have previously reported the synthesis and activity of a series of *N*-methyl-12-alkoxybenzo[*c*]phenanthridinium salts[15,19–21] and demonstrated that the introduction of short, aliphatic and non-functionalized 12-alkoxy groups produces the optimum results in different in vitro antileukemic activity assays. Of these derivatives, ethoxidine **3** demonstrated high cytotoxic activity on the P388 and K562 cancer cell lines and uniquely, had the ability to induce differentiation in K562 human cells.[20] Ethoxidine was also shown to be a DNA intercalator[15,21] but unlike fagaronine, it suppressed both topo I and camptothecin-dependent cleavage sites in sequence-specific manner; sites including A(+1) and T(−1) bases immediately adjacent to the strand cut were found to be suppressed much more effectively by ethoxidine.[15] Fagaronine can therefore be classed as a topo I poison, whilst ethoxidine is a topo I suppressor, which emphasizes the mechanistic dichotomy that arises from small changes in the substituent environment for these ligands. Moreover, because ethoxidine inhibits DNA relaxation at a concentration 10-fold lower than fagaronine,[21] the assignment of suppression to high levels of drug binding seen with other intercalators (and fagaronine at high concentrations) is not plausible in this case.

We report here the collation of earlier biophysical and biochemical findings concerning BCP binding[15,19–21] with molecular modeling techniques to propose how these two structurally similar BCPs have such different mechanisms of action against topo I. The publication of the crystal structure of human topo I in a covalent and non-covalent complex with a DNA substrate[22] has improved our understanding of the molecular events involved in DNA binding, strand scission, and religation, yet until recently, the absence of equivalent structural detail for the ternary complexes meant models proposed for ligand poisoning of topo I were speculative.[22,23] Now, with the publication of a number of ligand–DNA–topo I ternary complex crystal structures, including indenoisoquinolines,[10–12] an insight into how the structurally related BCPs exert their activity can be gained.

2. Results

2.1. Steered molecular dynamics as a method to explore intercalative binding

Previous modeling studies investigating the binding mode of intercalating ligands with DNA have predominantly relied on either manual docking of the ligand followed by molecular dynamics (MD) simulations to explore local conformational space,[24] or manual docking followed by manual translation and rotation of the ligand in the intercalation site to observe changes in binding energy.[25,26] Automated docking procedures use Monte Carlo or genetic algorithms followed by MD[27] to propose the most energetically favorable conformation of the ligand in the intercalation site, and have been developed for protein–ligand binding, rather than nucleic acids. In all cases, a complete search of conformational space within the binding site is not systematically explored, which increases the possibility of important binding orientations being overlooked. We have developed an efficient and simple method to create a torque to conduct such a search of the available space within an intercalation site using steered molecular dynamics (SMD) based on the principles outlined in our recently published in silico footprinting methodology,[28] and can be used to investigate any intercalative complex in double, triple stranded or tetraplex DNA.

To establish the preferred binding orientations for fagaronine and ethoxidine within the DNA prior to binding with topo I, we needed to automate the movement of the ligand through 360° within the intercalation site. It was important that the ligand should not move as a rigid body and that the DNA bases in contact with the ligand should have enough flexibility to adapt to the ligand's changing orientation and therefore allow it to rotate without energetically insurmountable steric hindrance. Suitable DNA starting co-ordinates were obtained either directly using a crystal structure of the DNA from a topo I complex, or the required sequence was built using standardized B-DNA parameters.

If an intercalation site was not already evident from the crystal structure, it was inserted using standard methods detailed in Section 4. Each ligand had to be docked twice, in either a 'face-up' or 'face-down' orientation prior to initiating SMD, due to the asymmetric nature of the BCPs within the chiral DNA environment. The water and ions were removed before initiating the MD simulation and charges were removed from the DNA to facilitate movement.[28]

The 360° rotation within the intercalation site was achieved in stages using four fixed dummy atoms placed on the plane of the docked ligand (Fig. 1). Each dummy atom is used in turn as an anchor for quadratic angle restraints, which produce the force required for the

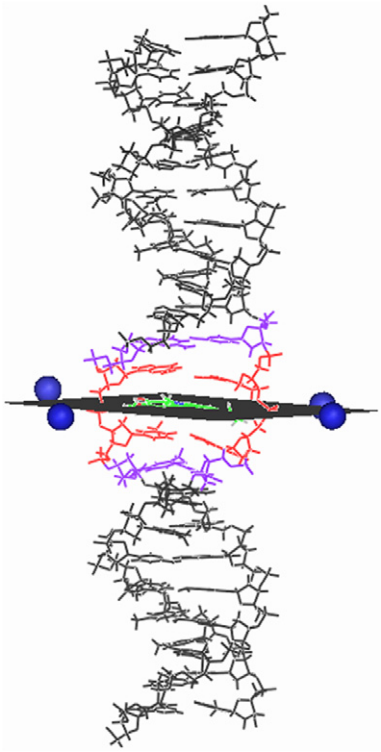

Figure 1. 22-mer DNA with **1** docked in the intercalation site, the plane of the dummy atoms is highlighted with the grey square, the bases in black remain fixed during the simulation, those in purple have 100 kcal mol^{-1} restraint and red have 10 kcal mol^{-1} restraint.

ligand to rotate in the MD simulation of the system (Fig. 2). To prevent the ligand from straying too far out of the intercalation site, a tether restraint was applied to the central carbon atom (C11a) in the ligand's fused ring system. The base pairs directly above and below the docked ligand were weakly restrained with a tether of 10 kcal mol^{-1} and each of the two contiguous base pairs was restrained more heavily (100 kcal mol^{-1}, Fig. 1) whilst the remaining DNA was fixed. An example of this SMD approach can be viewed in the movie file (fagaronine.avi) in the Supplementary Information.

Successful rotation and translation was achieved by carrying out MD simulations and by utilizing a combination of restraints, with coordinates saved into a trajectory file every 10 fs (further details for each ligand and starting orientation can be found in Section 4). Charges were reassigned to the DNA and the final dynamics trajectory was minimized with respect to the atomic coordinates. Visual inspection showed that the ligand had comprehensively explored the intercalation site (Fig. 3). Analysis of the minimized trajectory allowed the identification of the lowest energy conformation of the ligand within the DNA intercalative site, thus enabling identification of the preferred ligand binding orientation. In addition to the BCPs under investigation, we applied our SMD approach to the indenoisoquinoline **2b** for which a topo I complex structure is available[6] to validate the methodology.

2.2. Fagaronine binding with DNA

There are no definitive published data establishing the absolute binding orientation of the BCPs to DNA alone, other than implications that fagaronine binds with its iminium bond, or ethoxidine with its 12-ethoxy group, in the minor groove. The recently published crystal structure of topo I in the presence of a known poison, the structurally related indenoisoquinoline Mj-II-38 (PDB code; 1SC7[13]), was used for the model system to investigate binding of fagaronine. To first establish the preferred binding orientation with the nucleic acid substrate, DNA corresponding to the sequence in the ternary complex crystal structure was built and modified to incorporate an intercalation site at the same position as that in the crystal structure (see Section 4). The ligand was docked in each of the parallel orientations (**1a** and **1b**) prior to initiating SMD, and the minimized trajectory files in both orientations were analyzed by plotting the angle of rotation of the ligand in each minimized frame against the potential energy of the complex (Fig. 4). The dihedral angle descriptor (see Section 4) was chosen to represent the rotation of the ligand through 360°.

To compute the binding enthalpies (E_{bind}) for the most stable complexes identified by the SMD, the potential energies of the free DNA (without intercalation gap) and free ligand were summed then subtracted from the potential energy of the complex itself (Table 1, Eq. 1). Such a calculation provides information about the non-bonded contribution to complexation and the internal strains on both ligand and receptor induced through the binding event.[29] The E_{bind} values for **1a** and **1b** were −25.49 and −43.72 kcal mol^{-1}, respectively (Table 1).

The lowest energy intercalation complex observed is with orientation **1b**, where fagaronine forms a hydrogen

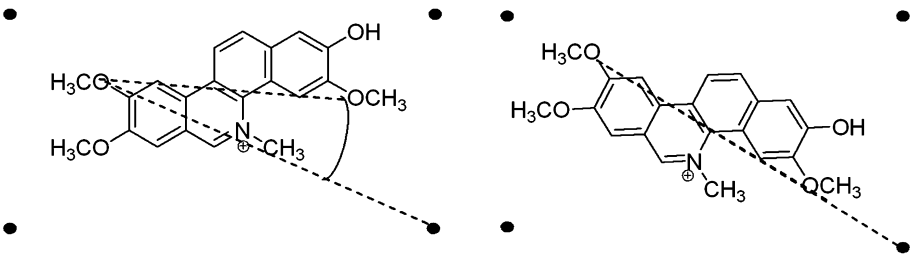

Figure 2. Fagaronine placed centrally relative to four dummy atoms. By setting the angle (3-*O*CH$_3$)–(9-*O*CH$_3$)–dummy atom restraint to 0° in the MD simulation, fagaronine can be rotated from its initial orientation (left) to that on the right. Changing the dummy atom anchor in subsequent steps allows complete rotation of the molecule.

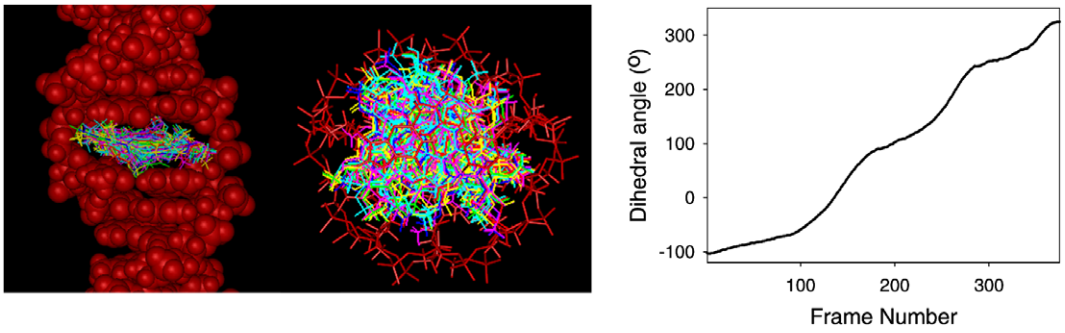

Figure 3. Intercalation site containing every 10th ligand conformation saved in the trajectory file shown from the side and above to illustrate the extensive nature of the search using SMD, and graphically to show all angular space has been covered.

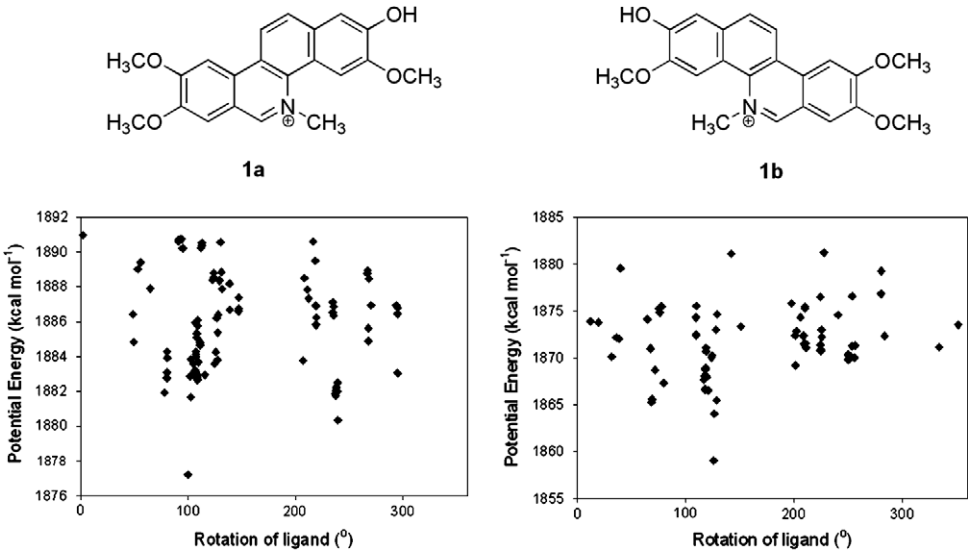

Figure 4. Potential energy for **1a** and **1b** complexed with DNA versus dihedral angle descriptor for rotation. All structures are from the post-minimized trajectories.

Table 1. E_{bind} values determined for fagaronine and ethoxidine binding to DNA using Eq. 1

	E_{bind}	=	$E_{complex}$	−	(E_{DNA}	+	E_{ligand})	(1)
1a	−25.49		1871.59		1490.58		406.50	
1b	−43.72		1853.36		1490.58		406.50	
3a	−50.68		1741.77		1365.57		426.88	
3b	4.43		1796.88		1365.57		426.88	

bond with the oxygen of the ribosyl ring of the lower base (Fig. 5). The low energy conformation for **1a** does not appear to form any H-bonds with DNA. In orientation **1a**, the ligand is approximately parallel in relation to the DNA base pairs above and below the intercalation site, with the iminium group pointing into the minor groove (data not shown), whereas **1b** prefers to adopt an almost parallel orientation with the OH and iminium group in the minor groove, similar to the 'mixed-mode' binding reported for protoberberine analogues whose chemical structures are similar to that of **1**.[25] Previously, biophysical measurements of fagaronine and CT DNA using surface-enhanced Raman spectroscopy (SERS) and flow linear dichroism spectroscopy (FLD)[15,21] demonstrated that the position of fagaronine relative to the DNA bases is almost parallel.[15,21] These techniques were not able to suggest the orientation of the quaternary nitrogen, but the authors proposed that both the OH group and the iminium group occupied the minor groove.[15,21] The SERS and FLD data imply that the OH group of **1** is involved in H-bonding, and could potentially be both an H-bond donor and acceptor. Our study confirms that in the preferred orientation of **1b**, which is almost parallel, an H-bond to the ribosyl oxygen of the base below the intercalation site can form, however, we could find no orientation where the 2-OH group could act as an acceptor, unless mediated through a water molecule. Nabiev and co-workers[15] proposed that an H-bond formed between the 2-OH group of fagaronine and the exocyclic NH_2 of the guanine base adjacent to the intercalation site, but our exhaustive search could only identify the ribose as an acceptor. The angle between the guanine amino group and the fagaronine OH was not conducive to H-bond formation throughout our simulation, which is not surprising, given the relative orientations of base pair to ligand in an intercalative event.

By means of UV spectrometry, Pezzuto et al. suggested that the quaternary nitrogen is directly involved in DNA binding inferred by a change in spectral shift that is not

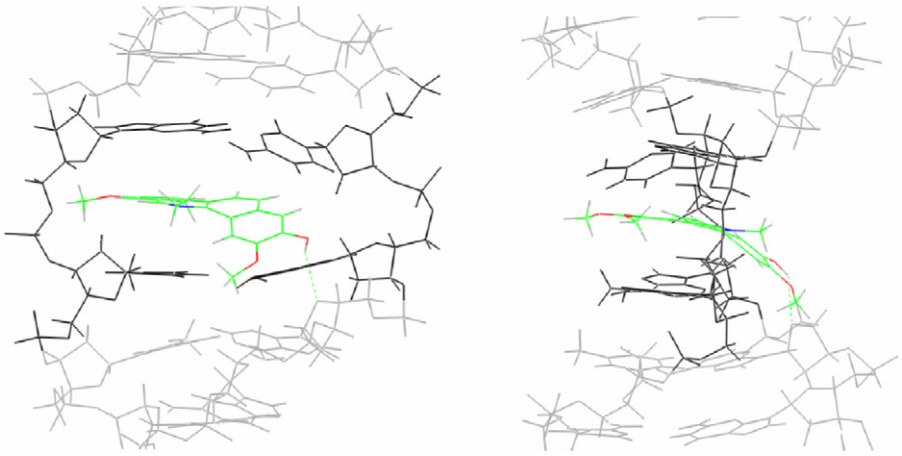

Figure 5. The lowest potential energy binding orientation of **1b** in the DNA sequence; the OH hydrogen bonds to the oxygen of the sugar moiety of the base below the intercalation site, with the N–CH_3 group pointing into the minor groove.

observed for norfagaronine. They proposed an ionic interaction between N^+ and the negatively charged phosphodiester backbone[30] as a binding mode. This did not correspond with any low energy orientations in our study, but it is equally possible for cationic groups to position themselves in the DNA grooves within the negative electrostatic field of DNA rather than being directly adjacent to the phosphate backbone[31,32] as seen with our models.

2.3. Fagaronine binding with topo I

The lowest energy fagaronine–DNA complexes identified by our SMD approach were inserted into the crystal structure solved for an indenoisoquinoline–DNA–topoI ternary complex (1SC7) by superimposition of the DNA coordinates from the simulation with those of the crystal, and the latter deleted. The RMS deviation of the residues and base pairs of the complex were not affected disadvantageously by the manipulation, with RMS deviations of 0.43 and 0.48 Å for the two orientations **1a** and **1b**, respectively. When we performed the equivalent manipulation with the indenoisoquinoline **2b** to which we had applied SMD within the DNA duplex removed from the crystal structure 1SC7, the ligand itself had an RMS deviation of 0.47 Å with the experimentally determined structure (tetracyclic ring atoms of the ligand), when our simulated low energy ligand–DNA complex was reinserted.

After the complex was solvated and minimized, the region of interest buried deep within the protein was subjected to simulated annealing (SA) followed by minimization to ensure residues involved in catalysis, binding, and stabilization had explored local conformational space and optimized their positions accordingly (Fig. 6).

The SA procedure applied to **1a** (Fig. 6a) infers that only significant movement occurs in the complex around the scissile guanine base and Arg 364. This is the residue that occupies the minor groove of the DNA and forms a key H-bond between the indenoisoquinoline **2b** and topo I in the crystal structure 1SC7. In the presence of **1a**, Arg 364 moves away from its original position defined by the crystal structure, and is accompanied by

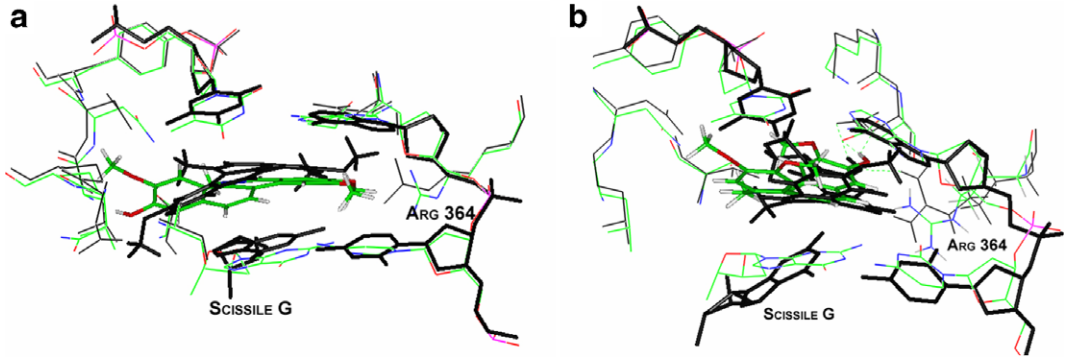

Figure 6. (a) Compound **1a** in topo I, residues and bases colored by atom type are post-minimization with **1a** (colored by atom, rendered), the black residues and bases highlight the positions adopted after annealing and subsequent minimization with **1a** rendered. Base pairs rendered are those above and below the ligand. (b) Compound **1b** in topo I, residues and bases colored by atom type are post-minimization with **1b** (colored by atom, rendered), the black residues and bases highlight the positions adopted after annealing and subsequent minimization with **1b** rendered, hydrogen bonds are shown by green dashed lines. Base pairs rendered are those above and below the ligand.

Table 2. E_{bind} values determined for fagaronine and ethoxidine binding to topo I/DNA using Eq. 2

	E_{bind}	=	$E_{complex}$	−	($E_{protein-DNA}$	+	E_{ligand})	(2)
1a	−172.91		−7671.55		−7905.14		406.50	
1b	−191.54		−7690.18		−7905.14		406.50	
3a	−155.22		−4990.28		−5261.94		426.88	
3b	−189.91		−5024.97		−5261.94		426.88	

significant movement with the scissile guanine base, which is not unexpected given the available space in this region of the major groove.

The SA procedure applied to **1b** (Fig. 6b) infers movement in the base pairs adjacent to the intercalation site, and the rearrangement of Arg 364 in the minor groove produces a hydrogen bond with the oxygen of the 2-OH group of **1**, and could be classed as equivalent to the interaction that stabilizes the complex between indenoisoquinoline and topo I in the crystal structure. Computation of the relative E_{bind} for orientations **1a** and **1b** (Table 2, Eq. 2) also confirms that the latter is the more favored arrangement in the complex (−172.91 and −191.54 kcal mol^{-1}, respectively).

2.4. Ethoxidine binding with DNA

In order to investigate the binding mode of **3**, a potent topo I suppressor that prevents the formation of the stable cleavable complex, we utilized the coordinates of a non-covalent binary complex of DNA with the Y723F mutant topo I (PDB code; 1A35[14]). The DNA from the crystal structure was extracted and modified to include an intercalation gap between the bases where the strand break would occur in the wild type complex, and provided the coordinates to investigate the preferred orientation of **3** within the DNA using SMD.

The lowest energy intercalation complex observed is with orientation **3a**, (Fig. 7) in which the ethoxidine bends down toward the adenine base below the intercalation gap. For both **3a** and **3b**, the ligand is approximately parallel, with the iminium group pointing into the major groove. The inherent twist in **3** forces the isoquinoline ring toward the adenine base below (**3b**) (data not shown) and above (**3a**) the intercalation site. The overall energy of the complex in orientation **3b** is significantly less favorable than that of orientation **3a** (Table 1). Whilst the interaction energies of the two orientations are comparable (−55.62 and −57.01 kcal mol^{-1} for **3a** and **3b**, respectively), the potential energies of the complexes in these orientations are very different (**3a**, 1741.77 kcal mol^{-1}; **3b**, 1796.88 kcal mol^{-1}) inferring that the DNA in orientation **3b** must adopt a high energy conformation to accommodate the ligand, which is reflected by the relative E_{bind} values for both complexes (−50.68 and 4.43 kcal mol^{-1}, respectively).

Biophysical measurements of ethoxidine and CT DNA using SERS and FLD[15,21] suggested that its position relative to the DNA bases is almost parallel.[15,21] Induced CD has shown that ethoxidine lies just off parallel with the DNA base pairs and that the bulky ethoxy substituent occupies the minor groove,[15] which our SMD approach has confirmed for **3a** (Fig. 8).

2.5. Ethoxidine binding with topo I

The lowest energy conformations of **3** within the DNA were replaced in the minimized topo I crystal structure (1A35) by superimposition of the intercalated DNA with that of the crystal structure (RMS values of 1.00 Å (**3a**) and 1.10 Å (**3b**) for DNA and 0.60 Å and 0.57 Å for protein backbone atoms, respectively). Although the intercalation gap produced an extension

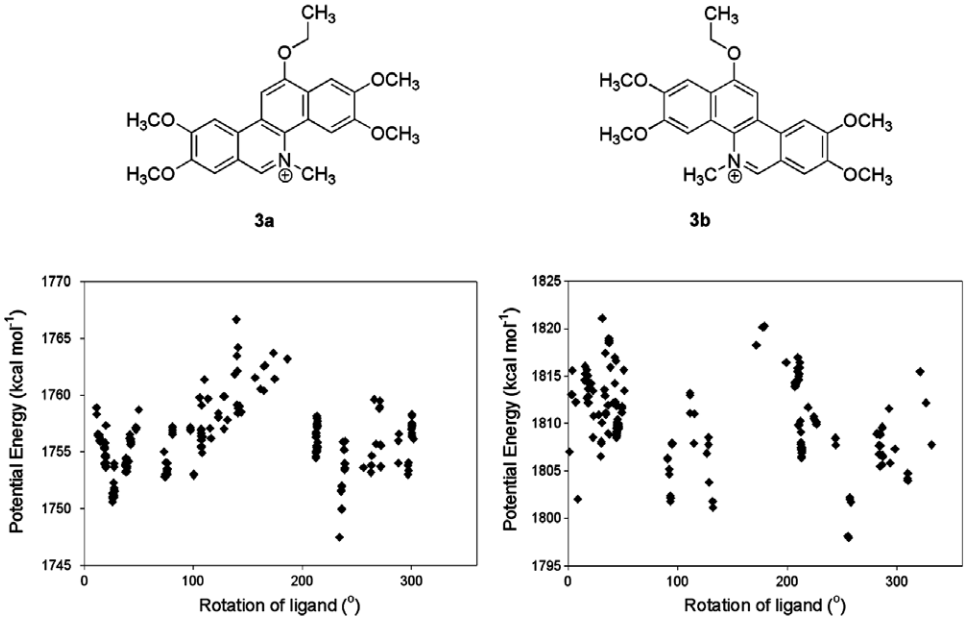

Figure 7. Potential energy for **3a** and **3b** complexed with DNA versus dihedral angle descriptor for rotation. All structures are from the post-minimized trajectories.

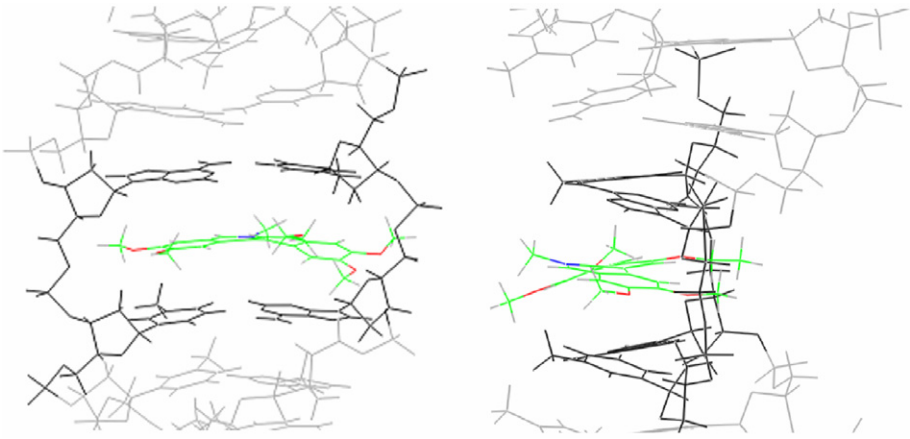

Figure 8. The lowest energy binding orientation of **3a** in the DNA sequence, the ethoxy group is positioned in the minor groove, the N–CH_3 group pointing into the major groove.

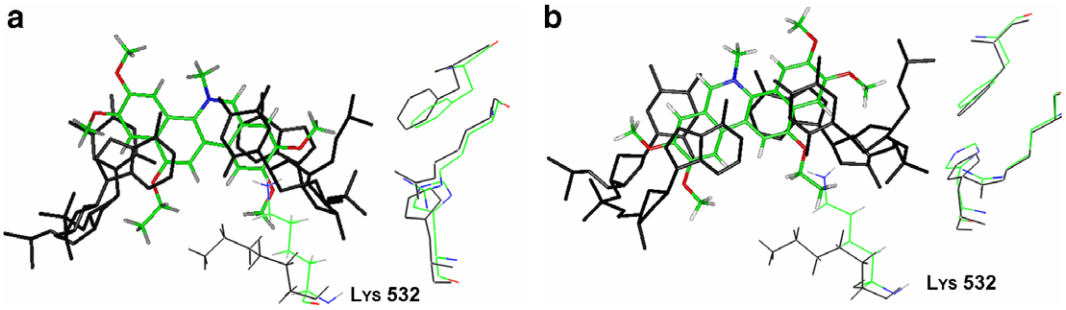

Figure 9. (a) Compound **3a** in topo I, residues and bases in black belong to the protein treated to simulated annealing, the residues colored by atom type belong to the minimized crystal structure, the ligand is in atom colors. (b) Compound **3b** in topo I, residues and bases in black belong to the protein treated to simulated annealing, the residues colored by atom type belong to the minimized crystal structure, the ligand is in atom colors.

to the DNA structure within the topo I central hole, an integrated H-bond network with the protein was re-established after minimization.

After SA of the binding region around **3a**, (Fig. 9a) there was little evidence of movement in the catalytic residues Tyr/Phe 723, His 632, and Arg 590, whereas Lys 532 underwent a significant change in position. SA of the binding region around **3b** (Fig. 9b) also showed little movement in the catalytic residues Tyr/Phe 723, His 632, and Arg 590, whereas Lys 532 demonstrates movement to a similar degree as the complex with **3a**. Whilst both orientations affect the relative positions of the catalytic residues to a similar extent, **3b** is predicted to be the more stable ternary complex (Table 2).

3. Discussion

In the absence of definitive crystal or NMR data for BCP binding with DNA, our SMD approach has exhaustively investigated fagaronine and ethoxidine binding and identified one favored orientation for each compound. Both low energy complexes comply with earlier biophysical experimental observations derived from spectroscopic measurements. Fagaronine adopts an almost parallel orientation with the iminium and OH groups in the minor groove, with the latter H-bonding to the DNA, whilst ethoxidine is also off-parallel, but with the iminium group lying in the major groove and the bulky 12-ethoxy group in the minor groove. Clearly, both BCPs have quite different orientations within the DNA, which has been repeatedly indicated in earlier studies.[15,19,21] Given that the BCPs are known to intercalate with DNA independently of topo I binding[15] (the active site is inaccessible in the topo I–DNA system) we propose that the low energy confomers we have identified are the most likely complexes that topo I will combine with. Our methodology predicted the correct orientation of the indenoisoquinoline **2b** both within the DNA and the topo I complex (1SC7) to an RMS deviation of 0.47 Å which helps substantiate our predictions.

In mechanistic terms, nucleophilic attack by the phenolic group of Tyr 723 of topo I on the scissile phosphate of the DNA strand requires base activation.[33–35] No crystal structures of topo I complexed with DNA (and ligands) have residues adjacent to Tyr 723 to fulfill this role, although a water molecule H-bonded to Arg 590 which is 2.3 Å from the phenolic group could act as a specific base if deprotonated[36] (Fig. 10). Arg 590 may also facilitate nucleophilic attack by stabilizing the phenolate of Tyr 723 when generated. Once Tyr 723 has attacked, there is a triad of basic amino acids (Arg 488, Arg 590, and His 632) positioned to stabilize the

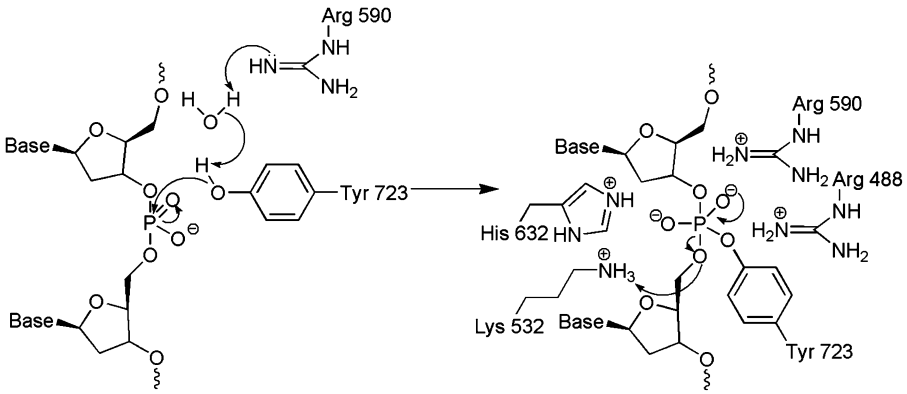

Figure 10. Phenolic attack on the scissile phosphate by Tyr 723 requires base activation, which leads to a pentavalent transition-state stabilized by a triad of basic residues. Lys 532 acts as an acidic proton donor to the 5-OH leaving group as cleavage occurs.

pentavalent transition-state through interactions with the non-bridging oxygens of the scissile phosphate (Fig. 10). A direct role in transition-state stabilization has also been implied for Lys 532,[37] but from the functional analysis of the topo I K532R and K532A mutants, it appears that Lys 532 acts as a general acid to protonate the leaving 5′-oxygen to drive the reaction to completion by creating an efficient leaving group.[39] Implicit to catalytic function is the attacking nucleophile and the three-dimensional organization of the side chains of the active site residues around the scissile phosphate in association with protonation of the 5′-OH during cleavage (Fig. 10).[38,39] Any disruption to the architecture of these residues would inevitably have profound effects on the ability of topo I to catalyze.

Both low energy complexes of fagaronine with DNA identified by SMD, when inserted back into topo I to re-establish the ternary complex derived from the crystal coordinates of the structure bound to an indenoisoquinoline, were stable when subjected to SA. All catalytic residues retained their positions, and conformer **1b** was able to switch its H-bond from the DNA ribose to Arg 364, an interaction deemed responsible for stabilizing the ternary complex with the indenoisoquinoline.[13] Retention of the integrity of the complex explains how fagaronine, like the indenoisoquinolines, is a topo I poison; the catalytic residues enable strand scission to occur, from nucleophilic attack through transition-state stabilization and protonation of the 5′-OH leaving group. Religation is prevented through the inability of the free 5′-OH to attack the phosphotyrosine, simply as a result of the distance introduced between the two groups (15.83 and 15.02 Å for **3a** and **3b**, respectively) by the intercalative event and the complex becomes trapped. Ethoxidine has only one realistic low energy complex with DNA as identified by SMD, which when inserted back into the topo I complex had a more significant effect on the positions of the catalytic residues compared to fagaronine. It has been suggested that ligand substitutions that impinge on the minor groove disfavor topo I poisoning activity,[40,41] which we suggest is the reason ethoxidine acts as a topo I suppressor rather than a poison. Extension of the 12-ethoxy group into the minor groove invoked little movement in Tyr/Phe 723 or the basic triad residues necessary for transition-state stabilization, but Lys 532 underwent a 2.43 Å displacement from the position necessary to act as a proton donor to facilitate cleavage. We therefore propose that ethoxidine acts as a suppressor rather than a poison because scission cannot occur when the catalytic residue responsible for generating an efficient leaving group is removed from the equilibrium. In the absence of a proton donor by the movement of Lys 532 out of position, there is no drive for strand scission to occur, and cleavage is suppressed. Indeed, Champoux and coworkers[37] demonstrated recently that they could only enable strand scission by the K532A topo I mutant by using a phosphorothiolate DNA oligonucleotide as a suicide substrate for the enzyme (5′-O replaced by 5′-S at the cleavage site). This alleviates the need for a general acid to protonate the leaving 5′-oxygen in the cleavage reaction because the thiolate anion, having a lower pK_a than the equivalent alkoxide, is stable and will facilitate the reaction. In this way, they were able to identify Lys 532 as essential for scission. Ethoxidine, by displacing Lys 532 from its role as a general acid, removes the drive for strand scission to occur because the 5′-oxygen cannot be stabilized by protonation, in contrast to fagaronine, where all catalytic residues can function normally to enable strand scission. Whilst the former suppresses topo I activity through preventing stand breakage in the first place, the latter is a poison, because after scission, religation cannot occur through misalignment, and the complex is trapped as a ternary complex.

4. Experimental

Atomic coordinates for the crystal structures of topo I were obtained from the Brookhaven Protein Databank[42] (PDB codes 1SC7,[13] 1A35[14]) and manipulated using Accelrys' InsightII program (Accelrys Inc., San Diego, CA) on a Silicon Graphics Octane2 workstation (2×600 MHz MIPS R14000 processors). The Discover3 simulation engine (Accelrys Inc., San Diego, CA) was used to perform all calculations employing the cff91 force field.[28]

4.1. Fagaronine—preparing the simulation

The crystal structure of topo I in the presence of an indenoisoquinoline poison (1SC7) was used as a model structure to investigate the preferred binding of fagaronine. The energy of the complex surrounded in a 5 Å layer of water was minimized with respect to its atomic coordinates and in a step-wise manner; the heavy atoms were fixed, allowing hydrogen atom positions to be optimized, followed by the side chains, before the full structure was allowed to relax. The cff91 forcefield was used for all energy calculations in conjunction with a distance dependent dielectric of 4.0 r_{ij} and non-bonded interaction cutoffs of 9.5 Å for van der Waals forces and 15 Å for electrostatic interactions. Minimization was carried out using a conjugate gradient (CG) algorithm until an energy convergence criterion of 0.1 kcal mol^{-1} Å^{-1} was satisfied.

The 22-mer strand of DNA in the crystal structure was constructed using standardized B-DNA helical parameters. Sodium counter ions were placed 5 Å from the oxygen atoms of the phosphate groups in order to maintain charge neutrality. The system was then solvated in layers of water and minimized using the convergence criteria described above. The potential energy of the DNA alone was calculated (without water and sodium ions) to provide a value for E_{DNA} (1490.58 kcal mol^{-1}) to use in the determination of E_{bind} described by Eq. 1 (Table 1).

To create an intercalation site in the DNA strand, the bonds between the 3′ oxygen and the phosphate on both sides were broken and the distance between the two base pairs adjacent to the site was increased from approximately 3.5 to 6.8 Å. The DNA bases were rotated through an angle of ~15° to mimic the unwinding characteristics of intercalation and religated.

Fagaronine was parameterized for the cff91 forcefield and atoms assigned ESP partial charges via MOPAC[18] using the AM1 Hamiltonian. Fagaronine was then minimized in a box of explicit water under periodic boundary conditions (25 × 15 × 20 Å). The energy of the ligand (E_{ligand}) was evaluated for use in the calculation of net binding enthalpies (Table 1). The minimized ligand was then manually docked into the intercalation site of the DNA in a parallel orientation and minimized with water and counter ions, as previously described. This procedure was repeated with fagaronine in the opposite parallel orientation.

4.2. Fagaronine—SMD exploration of DNA binding

Molecular dynamics simulations were performed in vacuo at 300 K using a distance dependent dielectric constant of 1.0 r_{ij}, with non-bonded interaction cutoffs of 9.5 Å for van der Waals interactions and 15 Å for electrostatic interactions. All simulations used a 1 fs timestep for durations specified in Table 3. DNA atoms had fixed Cartesian coordinates except the two base pairs directly adjacent to the ligand, which had a tether restraint applied to them with a force constant of 10 kcal mol^{-1} (Fig. 1) and the contiguous two base pairs in the sequence, which were subjected to a 100 kcal mol^{-1} tether restraint (Fig. 1). Different sets of restraints were required to rotate fagaronine through 360° in the plane of the base pairs depending on orientation (**1a**/**1b**; Table 3). Two distance restraints, each with a 100 kcal mol^{-1} force constant, were applied in two directions across the ligand, from O2′ to O8′, and O3′ to O9′, which was necessary to prevent the molecule from buckling from the angle restraint pulling the ligand while being rotated. Fagaronine was found to buckle and unrealistically distort in shape without these. Details of the restraints are given in Table 3 and shown schematically in Figure 11.

Table 3. The restraints used in the SMD simulation to rotate **1a**, **1b**, **3a**, and **3b** through 360° in the intercalation site

Molecule	Tether restraint (kcal mol^{-1})	Distance (Å)		Dummy atom	Angle restraint (kcal mol^{-1})	Number of steps
		$O^{2'}$–$O^{8'}$	$O^{3'}$–$O^{9'}$			
1a	70	11.2	12	1B	110	900
				1D	60	750
				1C	130	400
				1	120	800
				1D	120	900
1b	60	11.2	12	1	100	750
				1B	110	450
				1D	110	700
				1C	110	450
				1	100	500
3a	50	12	11	1D	40	2000
				1C	90	800
				1	110	1000
				1B	90	800
				1D	110	1000
3b	50	12	11	1	100	1000
				1B	110	500
				1D	100	1000
				1C	100	1000

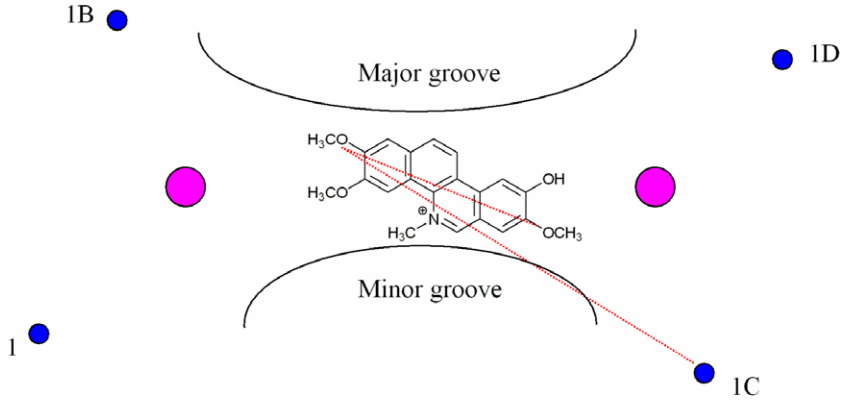

Figure 11. A schematic representation of the molecular dynamics simulation designed to rotate the BCP through 360°.

The molecular dynamics trajectory was captured by saving the structure of the complex every 10 fs of the simulation. Each structure in the trajectory file was then minimized in vacuo in a stepwise manner, gradually reducing the restraints of the tethered bases from 100 and 10 kcal mol^{-1} to the values shown in Table 4, until a derivative of 0.1 kcal mol^{-1} Å^{-1} was reached.

After minimizing the trajectory structures, the optimum binding orientation for fagaronine was determined by analyzing the graphical representation of the change in potential energy between the ligand and the DNA as a function of the dihedral angle C1′–C1′–C2–C8, where the C1′ atoms are those of the fixed base pairs, above the ligand and C2 and C8 are atoms of the ligand (Fig. 12).

To calculate E_{bind}, the potential energy of the minimized free DNA (E_{DNA}) was added to the potential energy of the minimized, free ligand (E_{ligand}) and subtracted from the potential energy of each of the low energy BCP complexes ($E_{complex}$) identified by the SMD simulation (Eq. 1, Table 1).

4.3. Fagaronine binding with topo I

The DNA conformation with the lowest energy identified by the SMD simulation was replaced in the minimized topo I crystal structure (1SC7) by superimposition of the DNA with that of the crystal structure. The complex was manually aligned using the base pairs above and below the ligand with the corresponding base pairs in the topo I complex, before minimization in a stepwise manner as previously described. Residues and DNA bases within 8 Å of the ligand were subjected to an annealing process of 300–270 K for 5 ps with a timestep of 1 fs, followed by a final minimization using the parameters previously described. The binding enthalpy was calculated for each topo I:**1** complex by subtracting the energy of the protein complex ($E_{complex}$) from the combined energy of the free ligand (E_{ligand}) and the covalent complex of the DNA and topo I without the intercalation gap ($E_{protein-DNA}$, Table 2). To determine the latter, DNA of the same sequence was built and minimized in the presence of water and sodium ions, then superimposed (heavy atoms) onto the six DNA bases below the indenoisoquinoline in the crystal structure. The phosphodiester backbone was cleaved and the corresponding bond formed with Y723, followed by capping of the scissile guanine base as in the crystal structure. The resulting structure was minimized in a layer of water and annealed as before.

Table 4. The stepwise restraint procedure used during the minimization of the trajectory files (see Fig. 1 where bases adjacent to gap are colored red and contiguous bases are colored purple)

Simulation	Restraints to bases adjacent to gap (kcal mol^{-1})	Restraints to contiguous bases (kcal mol^{-1})
Step 1	10	100
Step 2	10	50
Step 3	1	10
Step 4	0.5	1
Step 5	0.25	0.5
Step 6	0.1	0.2
Step 7	0.0	0.0

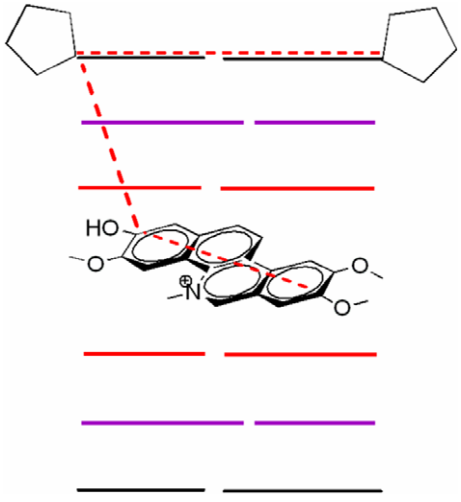

Figure 12. The atoms used to measure the change in dihedral angle throughout the simulation (red dashed line). The C1′ atoms of the sugars belong to the base pairs that remain fixed during the simulation in order to give a fixed point of reference for simpler analysis. The red base pairs have a 10 kcal mol^{-1} restraint throughout the simulation and the purple have 100 kcal mol^{-1} restraint throughout the simulation.

4.4. Ethoxidine—preparing the simulation

The crystal structure of topo I (Y723F mutant) in the presence of a 22-mer duplex of DNA (PDB code; 1A35[14]) was used as a model structure to investigate the preferred binding of ethoxidine. The complex was minimized applying the same protocol used for 1SC7.

The DNA was removed from the non-covalent binary complex crystal structure 1A35 and the bromouridine bases were modified to thymidine followed by minimization in layers of water, in the presence of sodium ions as previously described. The potential energy of the DNA alone was calculated (without water and sodium ions) to give a value for E_{DNA} to use in the determination of E_{bind} described by Eq. 1 (Table 1). The DNA was then modified to incorporate an intercalation site as for fagaronine.

Ethoxidine, with ESP partial charges, was then minimized in a box of explicit water as detailed for fagaronine. The minimized ligand was manually docked into the intercalation site in parallel orientations (**3a** and **3b**) and minimized in layers of water as previously described.

4.5. Ethoxidine—SMD exploration of DNA binding

Simulations were performed in vacuo at 300 K using the protocol described for fagaronine. Sets of restraints required to turn **3a** and **3b** through 360° are described in Table 3. As for fagaronine, a constant force (100 kcal mol^{-1}) was applied in two directions across the ligand from O2′ to O8′, and O3′ to O9′, which was necessary to prevent the molecule from buckling from the angle restraint pulling the ligand, with the restraint distance shown in Table 3.

All trajectories were obtained by saving the structure of the complex every 10 fs, followed by minimization of each structure in the trajectory file as described for fagaronine (Table 4). After minimizing the trajectory structures, the optimum binding orientation was determined by analyzing the graphical representation of the potential energies of the minimized trajectory structures against angular rotation.

To calculate E_{bind}, the potential energy of the minimized free DNA (E_{DNA}) was added to the potential energy of the free minimized ligand (E_{ligand}) and subtracted from the potential energy of each of the low energy BCP ($E_{complex}$) identified by the SMD simulation (Eq. 1, Table 1).

4.6. Ethoxidine binding with topo I

The lowest energy conformations of **3** in DNA were replaced in topo I (1A35) by superimposition of the intercalated DNA onto the DNA in the crystal structure. The original DNA from the crystal structure was deleted and the new complex was treated to minimization in a step-wise manner as previously described, after initially allowing the residues within 8 Å of the DNA to relax first to re-establish the H-bond network between protein and DNA previously lost through the introduction of an intercalation gap. The minimized structures maintained 14 hydrogen bonds and a further 16 new hydrogen bonds were formed between the DNA and the protein, totaling the same amount observed in the original crystal structure.

Simulated annealing was performed on the complexes using the protocol described for fagaronine. E_{bind} values are shown in Table 2.

Supplementary data

Supplementary data associated with this article can be found, in the online version, at doi:10.1016/j.bmc.2007.05.002.

References and notes

1. Stewart, L.; Redinbo, M. R.; Qui, X.; Hol, W. G. J.; Champoux, J. J. *Science* **1998**, *279*, 1534.
2. Hann, C.; Evans, D. L.; Fertala, J.; Benedetti, P.; Bjornsti, M.; Hall, D. J. *J. Biol. Chem.* **1998**, *14*, 8425.
3. Bendixen, C.; Thompsen, B.; Alsner, J.; Westergaard, O. *Biochemistry* **1990**, *29*, 5613.
4. Pourquier, P.; Pilon, A.; Kohlhagen, G.; Mazumder, A.; Sharma, M.; Pommier, Y. *J. Biol. Chem.* **1997**, *272*, 26441.
5. Staker, B. L.; Feese, M. D.; Cushman, M.; Pommier, Y.; Zembower, D.; Stewart, L.; Burgin, A. B. *J. Med. Chem.* **2005**, *48*, 2336.
6. Ioanoviciu, A.; Antony, S.; Pommier, Y.; Staker, B. L.; Stewart, L.; Cushman, M. *J. Med. Chem.* **2005**, *48*, 4803.
7. Simanek, V. In *The Alkaloids*; Brossi, A., Ed.; Academic Press Inc.: New York, 1985; Vol. 26, pp 185–240.
8. Pezzuto, J. M.; Antosiak, S. K.; Messmer, W. M.; Slaytor, M. B.; Honig, G. R. *Chem-Biol. Inter.* **1985**, *43*, 323.
9. Messmer, W. M.; Tin-Wa, M.; Fong, H. H.; Bevelle, C.; Farnsworth, N. R.; Abraham, D. J.; Trojanek, J. *J. Pharm. Sci.* **1972**, *61*, 1858.
10. Cushman, M.; Jayaraman, M.; Vroman, J. A.; Fukunaga, A. K.; Fox, B. M.; Kohlhagen, G.; Strumberg, D.; Pommier, Y. *J. Med. Chem.* **2000**, *43*, 3688.
11. Jayaraman, M.; Fox, B. M.; Hollingshead, M.; Kohlhagen, G.; Pommier, Y.; Cushman, M. *J. Med. Chem.* **2002**, *45*, 242.
12. Strumberg, D.; Pommier, Y.; Paull, K.; Jayaraman, M.; Nagafuji, P.; Cushman, M. *J. Med. Chem.* **1999**, *42*, 446.
13. Larsen, A. K.; Grondard, L.; Couprie, J.; De Soize, B.; Comoe, L.; Jardillier, J. C.; Riou, J. F. *Biochem. Pharmacol.* **1993**, *46*, 1403.
14. Wang, L. K.; Johnson, R. K.; Hechet, S. M. *Chem. Res. Toxicol.* **1993**, *6*, 813.
15. Fleury, F.; Sukhanova, A.; Ianoul, A.; Devy, J.; Kudelina, I.; Duval, O.; Alix, A. P. J.; Jardillier, J. C.; Nabiev, I. *J. Biol. Chem.* **2000**, *275*, 3501.
16. Wassermann, K.; Markovits, J.; Jaxel, C.; Capranico, C.; Kohn, K. W.; Pommier, Y. *Mol. Pharmacol.* **1990**, *38*, 38.
17. Pommier, Y.; Pourquier, P.; Fan, Y.; Strumberg, D. *Biochim. Biophys. Acta* **1998**, *1400*, 83.
18. Beerman, T. A.; McHugh, M. M.; Sigmund, R.; Lown, J. W.; Rao, K. E.; Bathini, Y. *Biochim. Biophys. Acta* **1992**, *1131*, 53.

19. Mackay, S. P.; Comoe, L.; Desoize, B.; Duval, O.; Jardillier, J. C.; Waigh, R. D. *Anti-Cancer Drug Des.* **1998**, *13*, 797.
20. Lynch, M. A.; Duval, O.; Sukhanova, A.; Devy, J.; Mackay, S. P.; Waigh, R. D.; Nabiev, I. *Bioorg. Med. Chem. Lett.* **2001**, *11*, 2643.
21. Ianoul, A.; Fleury, F.; Duval, O.; Waigh, R.; Jardillier, J. C.; Alix, A. J. P.; Nabiev, I. *J. Phys. Chem. B* **1999**, *103*, 2008.
22. Redinbo, M. R.; Stewart, L.; Kuhn, P.; Champoux, J. J.; Hol, W. G. *Science* **1998**, *279*, 1504.
23. Fan, Y.; Weinstein, J. N.; Kohn, K. W.; Shi, L. M.; Pommier, Y. *J. Med. Chem.* **1998**, *41*, 2216.
24. (a) Guyen, B.; Schultes, C. M.; Hazel, P.; Mann, J.; Neidle, S. *Org. Biomol. Chem.* **2004**, *2*, 981; (b) de Pascual-Teresa, B.; Gallego, J.; Ortiz, A. R.; Gago, F. *J. Med. Chem.* **1996**, *39*, 4810; (c) Braña, M. F.; Casarrubios, L.; Dominguez, G.; Fernandez, C.; Perez, J. M.; Quigora, A. G.; Navarro-Ranninger, C.; de Pascual-Teresa, B. *Eur. J. Med. Chem.* **2002**, *37*, 301; (d) Mazerski, J.; Muchewicz, K. *Acta Biochim. Pol.* **2000**, *47*, 65.
25. Pilch, D. S.; Yu, C.; Makhey, D.; LaVoie, E. J.; Srinivasan, A. R.; Olson, W. K.; Sauers, R. R.; Breslauer, K. J.; Geacintov, N. E.; Liu, L. F. *Biochemistry* **1997**, *36*, 12542.
26. Reha, D.; Kabelac, M.; Ryjacek, F.; Sponer, J.; Sponer, J. E.; Elstner, M.; Suhai, S.; Hobza, P. *J. Am. Chem. Soc.* **2002**, *124*, 3366.
27. Dheyongera, J. P.; Geldenhuys, W. J.; Dekker, T. G.; Van der Schyf, C. J. *Bioorg. Med. Chem.* **2005**, *13*, 689.
28. Anthony, N. G.; Huchet, G.; Johnston, B. F.; Parkinson, J. A.; Suckling, C. J.; Waigh, R. D.; Mackay, S. P. *J. Chem. Inf. Model.* **2005**, *45*, 1896.
29. Cairns, D.; Michalitsi, E.; Jenkins, T. C.; Mackay, S. P. *Bioorg. Med. Chem.* **2002**, *10*, 803.
30. Pezzuto, J. M.; Antosiak, S. K.; Messmer, W. M.; Slaytor, M. B.; Honig, G. R. *Chem. Biol. Interact.* **1983**, *43*, 323.
31. Jain, M.; Barthwal, S. K.; Barthwal, R.; Govil, G. *Arch. Biochem. Biophys.* **2005**, *439*, 12.
32. Barthwal, R.; Jain, M.; Awasthi, P.; Srivastava, N.; Sharma, U.; Kaur, M.; Govil, G. *J. Biomol. Struct. Dyn.* **2003**, *21*, 407.
33. Champoux, J. J. In *DNA Topology and its Biological Effects*; Wang, J. C., Cozzarelli, N. R., Eds.; Cold Spring Harbor Lab. Press: New York, 1990; pp 217–242.
34. Sherratt, D. J.; Wigley, D. B. *Cell* **1998**, *93*, 149.
35. Stivers, J. T.; Shuman, S.; Mildvan, A. S. *Biochemistry* **1994**, *33*, 15449.
36. Redinbo, M. R.; Champoux, J. J.; Hol, W. G. *Biochemistry* **2000**, *39*, 6832.
37. Interthal, H.; Quigley, P. M.; Hol, W. G.; Champoux, J. J. *J. Biol. Chem.* **2004**, *279*, 2984.
38. Lisby, M.; Krogh, B. O.; Boege, F.; Westergaard, O.; Knudsen, B. R. *Biochemistry* **1998**, *37*, 10815.
39. Christiansen, K.; Knudsen, B. R.; Westergaard, O. *J. Biol. Chem.* **1994**, *269*, 11367.
40. Mackay, S. P.; Meth-Cohn, O.; Waigh, R. D. *Adv. Heterocycl. Chem.* **1996**, *67*, 345.
41. Kerry, M. A.; Duval, O.; Waigh, R. D.; Mackay, S. P. *J. Pharm. Pharmacol.* **1998**, *50*, 1307.
42. Berman, H. M.; Henrick, K.; Nakamura, H. *Nat. Struct. Biol.* **2003**, *10*, 980.